

Macroscopic Quantum Coherence in Molecular Magnets

Alain Chiolero and Daniel Loss

Department of Physics and Astronomy, University of Basel, Klingelbergstrasse 82, 4056 Basel, Switzerland
(Received 28 July 1997)

We study macroscopic quantum coherence in antiferromagnetic molecular magnets in the presence of magnetic fields. Such fields generate artificial tunnel barriers with externally tunable strength. We give detailed semiclassical predictions for tunnel splitting in various regimes for low and high magnetic fields. We show that the tunneling dynamics of the Néel vector can be directly measured via the static magnetization and the specific heat. We also report on a new quantum phase arising from fluctuations. The analytic results are complemented by numerical simulations. [S0031-9007(97)04930-2]

PACS numbers: 75.10.Jm, 03.65.Sq, 73.40.Gk, 75.30.Gw

Quantum spin dynamics in mesoscopic magnets has received much attention over the recent years, both from experiment and from theory [1]. A number of nanosized particles in the superparamagnetic regime have been identified as promising candidates for the observation of macroscopic quantum phenomena (MQP) such as the tunneling of the magnetization out of a metastable potential minimum, or, more strikingly, macroscopic quantum coherence (MQC), where the magnetization (or the Néel vector) tunnels coherently between classically degenerate directions over many periods. On the one hand, these phenomena are interesting from a fundamental point of view as they extend our understanding of the transition from quantum to classical behavior. On the other hand, the measurement of MQP quantities such as the tunnel splitting provides independent information about microscopic parameters such as anisotropies and exchange constants.

A prominent example of such MQC behavior that has attracted wide attention is the antiferromagnetic ferritin [2]. More recently, molecular magnets [3] such as the ferric wheel or Mn_{12} have emerged as promising candidates for the experimental observation of MQP [4,5] mainly for three reasons. First, molecular magnets have well-defined structures and magnetic properties. Thus, precise values for the tunneling rates can be calculated. Second, molecular magnets can be produced as single crystals that contain a macroscopic number of identical magnetic subunits that are weakly coupled to each other as well as to their surroundings, as evidenced, e.g., by the observed MQP in Mn_{12} . Thus the amplification of the single-unit signal is naturally provided. Third, the typically high symmetry of these magnets reduces the number of independent parameters.

In this Letter we discuss novel tunneling scenarios in antiferromagnetic (AFM) molecular magnets. A key feature of our discussion is to exploit the well-known fact that an effective anisotropy can be generated in an AFM by applying a magnetic field. Thus it is possible to create tunnel barriers that are tunable by an external parameter. Evidently, such control parameters are highly desirable as they open the door to systematic tests of MQC. We concentrate on ringlike structures such as Fe_6 , Fe_{10} , and V_8 [3],

where the spins interact with their nearest neighbors via exchange coupling. In particular, we show that the tunneling rates become field dependent and thus can be measured via the static magnetization and (less surprisingly) also via the Schottky anomaly of the specific heat. Our discussion is based on the nonlinear sigma model (NLsM) that includes anisotropies and magnetic fields [6]. The quantum dynamics of the Néel vector is then studied by instanton methods. Such methods are semiclassical in nature, i.e., valid for large spins and in the continuum limit. To cover the small end of the size scale, we performed *ab initio* numerical calculations; they agree well with the analytic results in the regime where a comparison is possible. We find several distinct tunneling regimes, depending on the ratio of crystalline anisotropy to magnetic field. Motivated by recent measurements on single-crystal Fe_{10} which indicate the presence of an anisotropy axis [7], we give estimates of these MQC corrections in the magnetization and the specific heat, and we show that they are within experimental reach.

We consider a ringlike molecular magnet, modeled as N spins s regularly spaced on a circle lying in the xy plane, with N even. The Hamiltonian is ($\mathbf{S}_{N+1} \equiv \mathbf{S}_1$)

$$H = J \sum_i \mathbf{S}_i \cdot \mathbf{S}_{i+1} + \sum_i U_i(\mathbf{S}_i) + \hbar \mathbf{h} \cdot \sum_i \mathbf{S}_i, \quad (1)$$

with AFM exchange coupling $J > 0$, and where $U_i(\mathbf{S}_i)$ is the crystalline anisotropy at site i , $\mathbf{h} = \gamma \mathbf{B}$, with \mathbf{B} being the magnetic field, $\gamma = g \mu_B / \hbar$, and g is the electronic g factor. For simplicity, we assume that both g and J are isotropic, and that the point symmetry of the molecule is that of a ring. Up to second order in the spin variables, the most general form of the anisotropies is then $U_i(\mathbf{S}_i) = \tilde{k}_z S_{i,z}^2 + \tilde{k}_r (\mathbf{S}_i \cdot \mathbf{e}_i)^2$, where \tilde{k}_z and \tilde{k}_r are the axial and radial anisotropies, respectively, and \mathbf{e}_i is a unit vector at site i pointing radially outwards. We also assume that $J \gg \tilde{k}_z, \tilde{k}_r$, which is typically the case.

We now derive an effective Lagrangian (NLsM) describing the low-energy physics of (1) by extending standard techniques [8] to include magnetic fields. We introduce spin coherent states, and decompose the local spin as $\mathbf{S}_i = (-1)^i s \mathbf{n} + \mathbf{I}_i$, where the Néel vector \mathbf{n} (with

$\mathbf{n}^2 = 1$) is taken as uniform for our small system, and \mathbf{l}_i is the fluctuation at site i (with $\mathbf{l}_i \cdot \mathbf{n} = 0$). After integrating out the \mathbf{l}_i [9], and keeping only the lowest-order terms in \tilde{k}_z/J and \tilde{k}_r/J , we obtain the Euclidean Lagrangian [6]

$$L_E = \frac{N\hbar^2}{8J} [-(i\mathbf{n} \times \dot{\mathbf{n}} - \mathbf{h})^2 + (\mathbf{h} \cdot \mathbf{n})^2] + Nk_z s^2 n_z^2, \quad (2)$$

with a single effective axial anisotropy $k_z = \tilde{k}_z - \tilde{k}_r/2$. Note that the magnetic field has two effects. First, it creates a hard axis anisotropy along its direction. This is easy to interpret: The spins can gain Zeeman energy by canting towards the magnetic field, and this effect is maximal when the Néel vector is perpendicular to the field. What makes this anisotropy interesting for our purposes is that it is tunable by an external field. Second, a phase factor arises from the cross term $2i\mathbf{h} \cdot (\mathbf{n} \times \dot{\mathbf{n}})$. It will have important consequences at high fields.

Depending on the sign of k_z and on the orientation of the field, various scenarios can be envisaged [10]. For lack of space we restrict ourselves to the most interesting case where the field is in the ring plane, $\mathbf{B} = (B_x, 0, 0)$, and perpendicular to a hard axis, i.e., $k_z > 0$. The potential energy has then two minima at $\mathbf{n} = \pm \mathbf{e}_y$. Tunneling of the Néel vector between these classically degenerate states results in a tunnel splitting of the ground state energy, which can be calculated using instanton methods. For the semiclassical dynamics two kinds of hard axis anisotropies compete, the crystalline one, $Nk_z s^2$, and that induced by the field, $N(g\mu_B B_x)^2/8J$. Let us introduce their ratio $\lambda = 8s^2 J k_z / (g\mu_B B_x)^2$. For low fields ($\lambda \gg 1$), the hard axis is the z axis, and the Néel vector, staying close to the xy plane, tunnels via the x axis. For high fields ($\lambda \ll 1$) on the other hand, the hard axis is the x axis, and the Néel vector tunnels via the z axis while staying in the yz plane. Without the phase term $2i\mathbf{h} \cdot (\mathbf{n} \times \dot{\mathbf{n}})$ in (2), the crossover would occur for $\lambda = 1$, i.e., for a field $B_x = s\sqrt{8Jk_z}/g\mu_B$. As we will see, this extra term reduces the critical field.

We first concentrate on the high-field regime ($\lambda \ll 1$). In this case, the Néel vector is conveniently parametrized as $\mathbf{n} = (\cos \theta, \sin \theta \sin \phi, \sin \theta \cos \phi)$. We then find that the instanton solution minimizing the action belonging to (2) moves in the yz plane [11] with the frequency $\omega_{\text{hf}} = s\sqrt{8Jk_z}/\hbar$, and action

$$S_{\text{hf}}/\hbar = Ns\sqrt{2k_z/J} \pm i\pi \frac{Ng\mu_B B_x}{4J}, \quad (3)$$

where the upper and lower signs correspond to instantons and anti-instantons, respectively. Note that both the tunneling barrier and the attempt frequency are constant. The phase term in Eq. (3) arises because the spins cant towards the field, thereby acquiring an additional geometric phase factor.

For the calculation of the fluctuation determinants, it is convenient to pass to dimensionless variables in (2).

We write the action as $S = \hbar Ng\mu_B B_x/8J \int d\tilde{\tau} (\tilde{L} - h_x)$, with

$$\begin{aligned} \hbar\omega_{\text{lf}} &= g\mu_B B_x, \\ \tilde{L} &= \dot{\mathbf{n}}^2 + 2i(\mathbf{n} \times \dot{\mathbf{n}})_x + n_x^2 + \lambda n_z^2, \end{aligned} \quad (4)$$

where time is rescaled as $\tilde{\tau} = \omega_{\text{lf}}\tau$. Expanding around the instanton solution up to second order, one sees that the θ and ϕ fluctuations are decoupled. For the θ -fluctuation determinant we find in leading order $\exp\{\pm i\frac{\pi}{2} + \mathcal{O}(\lambda^{3/2})\}$. This is a new quantum phase distinguishing instantons from anti-instantons. Its occurrence is surprising, because it is due to quantum *fluctuations*, and not due to a topological term in the action, in marked contrast to phases arising usually in spin problems [8,12]. Moreover, this new quantum phase does *not* depend on the spin s . The fluctuation determinant for ϕ is standard, and by summing over all configurations [12], we finally find for the tunnel splitting of the ground state in the high-field regime,

$$\Delta_{\text{hf}} = 8\hbar\omega_{\text{hf}} \sqrt{\frac{\text{Re } S_{\text{hf}}}{2\pi\hbar}} e^{-\text{Re } S_{\text{hf}}/\hbar} \left| \sin\left(\frac{\pi}{2} \frac{Ng\mu_B B_x}{2J}\right) \right|. \quad (5)$$

Note that the tunnel splitting oscillates with the B field as a result of interference between quantum spin phases (the new additional phase induces a shift from the usual cosine [12] to a sine). Similar oscillations have been found in biaxial FM [13] and uniaxial AFM [14]; note, however, that in the latter work the fluctuation-induced phase shift identified here has been overlooked. Our results, including the phase shift, are fully confirmed by independent numerics (see below and Fig. 2).

Next, we consider the low-field regime ($\lambda \gg 1$), where we use the parametrization $\mathbf{n} = (\sin \theta \cos \phi, \sin \theta \sin \phi, \cos \theta)$. We start by integrating out the θ fluctuations to obtain an effective action. The term $(\mathbf{n} \times \dot{\mathbf{n}})_x$ in the Lagrangian (4) forces the instantons out of the xy plane. However, for $\lambda \gg 1$ the deviations are small. Thus, we write $\theta = \pi/2 + \vartheta$, and expand the Lagrangian to second order in ϑ . This gives $\tilde{L} \approx \dot{\phi}^2 + \cos^2 \phi + 4i\vartheta \dot{\phi} \cos \phi + \vartheta G \vartheta$, where $G = -\partial_{\tilde{\tau}}^2 + \lambda - \cos^2 \phi - \dot{\phi}^2$. Integrating out ϑ is now straightforward. For $\lambda \gg 1$ we find [15] that $G \approx \lambda$. Hence, we end up with the effective Lagrangian

$$\tilde{L}_{\text{eff}} = \left(1 + \frac{4}{\lambda} \cos^2 \phi\right) \dot{\phi}^2 + \cos^2 \phi. \quad (6)$$

A simple quadrature shows that the instantons of this Lagrangian have an action $\tilde{S}_{\text{eff}} = 4[1 + 4/3\lambda + \mathcal{O}(\lambda^{-2})]$. Reinstating full units, we finally get for the action in the low-field regime (neglecting corrections of order λ^{-2})

$$S_{\text{lf}}/\hbar = N \frac{g\mu_B B_x}{2J} \left(1 + \frac{1}{6} \frac{(g\mu_B B_x)^2}{s^2 J k_z}\right). \quad (7)$$

Comparison with Eq. (3) shows that the crossover between the low- and high-field regimes occurs for a magnetic field $B_x = \alpha s \sqrt{8Jk_z} / g\mu_B$, with $\alpha = [(3 + \sqrt{10})^{1/3} - (3 + \sqrt{10})^{-1/3}] / 2 \approx 0.64$, a sizable reduction over the result that would follow from neglecting the phase term $2i\mathbf{h} \cdot (\mathbf{n} \times \dot{\mathbf{n}})$ in (2).

Next we determine the fluctuation determinant. This raises one problem. While the action for the instanton solutions of (6) is easy to calculate, the solutions themselves cannot be obtained analytically. However, being interested only in the regime $\lambda \gg 1$, we can approximate this determinant by the one obtained for the fluctuations around the instantons of the Lagrangian $\bar{L} = \dot{\phi}^2 + \cos^2 \phi$. This results in

$$\Delta_{\text{If}} = 8\hbar\omega_{\text{If}} \sqrt{\frac{S_{\text{If}}}{2\pi\hbar}} e^{-S_{\text{If}}/\hbar}. \quad (8)$$

The low-field splitting decreases (roughly) exponentially with the field. This is easily interpreted: The tunneling barrier increases quadratically with the field, whereas the attempt frequency increases linearly.

We complete our derivation by discussing the range of validity of our results. A necessary condition to have tunneling (in the ground state) is that the barrier ΔU be much larger than half the attempt frequency ω [16]. Application of this criterion to the low- and high-field regimes yields two conditions, $g\mu_B B_x \gg 4J/N$, and $Ns\sqrt{k_z}/2J \gg 1$. The effective Lagrangian (2) was derived under the assumption of (local) Néel order. Hence, the Zeeman energy must be smaller than the exchange energy, i.e., $g\mu_B B_x \ll 4Js$. Finally, our expression for high-field tunnel splitting is valid for $\lambda \ll 1$, i.e., for $g\mu_B B_x \gg s\sqrt{8Jk_z}$, whereas the low-field predictions hold if $\lambda \gg 1$, i.e., for $g\mu_B B_x \ll s\sqrt{8Jk_z}$. We summarize in Fig. 1 the various regimes and critical fields we have obtained.

We now turn to the question of how to observe the tunnel splitting. In contrast to previous cases [17] such as ferritin [2] it is not possible to observe the switching of the Néel vector via an excess spin, since even if such an excess moment were present, it is easily seen [10] that it would always point along the magnetic field and not along the Néel vector. However, the dynamics of the Néel vector could be observed via resonances (occurring at Δ) in the NMR spectrum, which provides local spin information. An entirely different approach, which is possible only because the tunnel splitting is B -field dependent, is to measure the static magnetization $\mathbf{M} = -\langle g\mu_B \sum_i \mathbf{S}_i \rangle$ as a

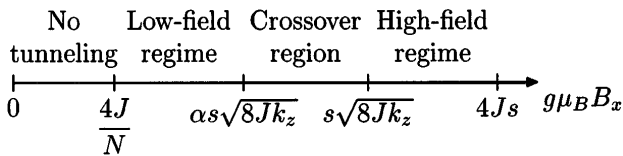


FIG. 1. Summary of the various regimes we have obtained as functions of the applied magnetic field ($\alpha \approx 0.64$).

function of applied field. Indeed, we have seen that the two lowest energy levels are tunnel split by Δ and are separated from the other levels by an energy $\hbar\omega \gg \Delta$, where Δ and ω are approximated by Δ_{lf} , Δ_{hf} , and ω_{lf} , ω_{hf} , respectively, depending on the field. At low temperatures, such that $k_B T \ll \hbar\omega$, the magnetization along the x axis is then found to be

$$M_x = \left(\frac{N}{8J} g\mu_B B_x - \frac{1}{2} \right) g\mu_B + \frac{\Delta'}{2} \tanh\left(\frac{\Delta}{2k_B T} \right). \quad (9)$$

Note that the first two terms in Eq. (9) give only a linear dependence on B_x . The last term shows that deviations are proportional to $\Delta' = \partial\Delta/\partial B_x$.

The tunnel splitting is also reflected in other thermodynamic quantities. For example, the low temperature specific heat exhibits a characteristic Schottky anomaly, $c_V = k_B (\Delta/2k_B T)^2 \text{sech}^2(\Delta/2k_B T)$, with a peak of height $0.64k_B$ at a temperature $T \approx 0.6\Delta/k_B$. The location of this peak thus gives the tunnel splitting.

The Lagrangian (2) is not limited to the tunneling regime, but also covers the nearly free limit of small k_z , such that $Ns\sqrt{k_z}/2J \ll 1$. This regime is most conveniently studied in terms of the corresponding Hamiltonian which is of rigid rotor type, $H_{\text{rot}} = \frac{2J}{N\hbar^2} \mathbf{L}^2 + \gamma \mathbf{L} \cdot \mathbf{B} + Nk_z s^2 n_z^2$, where \mathbf{n} and the angular momentum \mathbf{L} satisfy standard commutation relations $[L_j, n_k] = i\hbar \epsilon_{jkl} n_l$. For $k_z = 0$, the ground state is the state $|l, l\rangle$, with $l = [g\mu_B B_x N / 4J]$. Hence, the magnetization $M_x = lg\mu_B$ consists of steps of height $g\mu_B$, occurring with a period $g\mu_B \Delta B_x = 4J/N$ [18]. This agrees with previous results obtained in the absence of anisotropies and tunneling [3]. A small value of k_z (before tunneling sets in) leads to a rounding of the steps, as is easily seen from perturbation theory. For larger k_z such that $\Delta \ll \hbar\omega$ the Néel vector no longer freely rotates but becomes strongly localized along the easy axis. As a consequence, the steps in the magnetization vanish; see (9). Conversely, notice that whatever the value of $k_z \ll J$ sharp steps are recovered if the magnetic field is applied *along* the hard axis. We have also confirmed this picture by direct numerical diagonalization of H_{rot} .

The semiclassical analysis presented so far applies strictly speaking only to a sizable number of spins with $s \gg 1$. However, as is often the case with such methods the results are valid (at least qualitatively) even down to a few spins of small size. This expectation is indeed confirmed by direct numerical simulations which we have performed on Hamiltonian (1). Results for $N = 4$ and $s = 5/2$, and for some typical values $\tilde{k}_z = J/10$, and $\tilde{k}_r = 0$, are presented in Fig. 2. We note that since most symmetries are broken in (1), larger system sizes become quickly inaccessible to numerics. The agreement with the semiclassical prediction is satisfactory in the high-field regime. Since for our test system the low-field regime

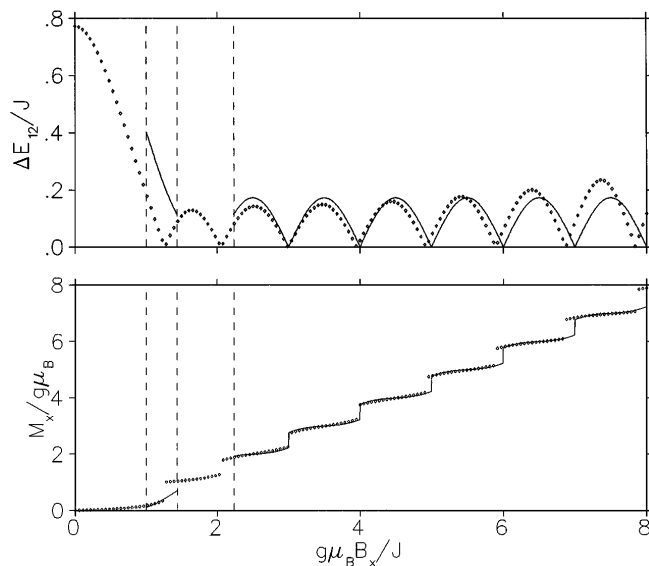


FIG. 2. Results for the energy splitting ΔE_{12} between the lowest two states (upper panel) and the magnetization M_x at $T = 0$ (lower panel) for a system of $N = 4$ spins $s = 5/2$ with $k_z = J/10$ and $k_r = 0$. The symbols give the results of a direct diagonalization of the Hamiltonian (1); the continuous lines give the semiclassical predictions. The dashed vertical lines indicate the various critical fields (see Fig. 1).

becomes vanishingly small, i.e., $1 \ll g\mu_B B_x/J \ll \sqrt{5}$, we cannot expect to find good quantitative agreement in this regime. Still, we can see from Fig. 2 that at the qualitative level the numerical and semiclassical approach show reasonable agreement. We have also calculated numerically the matrix elements of the staggered magnetization and could confirm the tunneling picture. Thus, our theoretical predictions give reasonably good results even for a very small cluster (and similarly for rings with larger N but smaller s [10]). Obviously, the accuracy of the semiclassical results will improve for larger systems.

To support the experimental relevance of our results, we give some estimates for the ferric wheel, Fe_{10} , for which $N = 10$, $s = 5/2$, $J/g\mu_B = 10$ T [3]. While magnetization measurements have been reported [3], no conclusive comparison with our theory is possible presently since they have been performed on polycrystalline samples with random orientation of the anisotropy axis, whereas the tunneling effect discussed here requires the B field to have a fixed orientation with respect to such an axis. However, from the well-defined steps that have been observed and from recent single-crystal measurements [7] one can infer that the magnitude of k_z/J is small, and of the order of 0.03 [7]. The low-field regime extends then from 4 to 7.8 T, with a tunnel splitting Δ_{1f}/h decaying exponentially from (roughly) 6×10^{10} to 4×10^9 Hz. Correspondingly, the Schottky peak of the specific heat shifts from 1.6 to 0.12 K, while the tunneling corrections in the magnetization range from 60% down to 16% of μ_B . The high-field regime starts at 12 T, with the tunnel splitting having oscillations of magnitude $\Delta_{hf}/h \approx 6 \times 10^9$ Hz and period 4 T. The

tunneling corrections in the magnetization reach at their peak 17% of μ_B . The Schottky peak oscillates between zero and 0.2 K. The crossover temperature to the quantum regime, $T_c = \hbar\omega/4k_B$, is in the 1–4 K range. Finally we remark that the same numbers apply to the high-field regime of an easy-axis system [10]. Hence, all quantities appear to be well within experimental reach [19].

We are grateful to D. D. Awschalom and J. Harris for useful discussions and for providing us with unpublished data. We also thank D. P. DiVincenzo and B. Pilawa for useful discussions. One of us (D. L.) is grateful for the hospitality of the ITP Santa Barbara (U.S. NSF Grant No. PHY94-07194), and of the INT Seattle, where part of this work was performed.

- [1] For an overview, see e.g., *Quantum Tunneling of Magnetization*, edited by L. Gunther and B. Barbara (Kluwer, Dordrecht, The Netherlands, 1994), and references therein.
- [2] D. D. Awschalom *et al.*, Phys. Rev. Lett. **68**, 3092 (1992); S. Gider *et al.*, Science **272**, 424 (1996).
- [3] D. Gatteschi, A. Caneschi, L. Pardi, and R. Sessoli, Science **265**, 1054 (1994).
- [4] J. R. Friedman *et al.*, Phys. Rev. Lett. **76**, 3830 (1996).
- [5] L. Thomas, F. Lioni, R. Ballou, D. Gatteschi, R. Sessoli, and B. Barbara, Nature (London) **383**, 145 (1996).
- [6] Similar Lagrangians have been used to study macroscopic magnets and spin chains. See, e.g., A. F. Andreev and V. I. Marchenko, Sov. Phys. Usp. **23**, 21 (1980); H. J. Mikeska, J. Phys. C **13**, 2913 (1980).
- [7] J. Harris and D. D. Awschalom (private communication).
- [8] E. Fradkin, *Field Theories of Condensed Matter Systems* (Addison-Wesley, Reading, MA, 1991).
- [9] Note that due to the magnetic field special care must be given to the constraint $\mathbf{n} \cdot \mathbf{l}_i = 0$.
- [10] A. Chiolerio and D. Loss (to be published).
- [11] Since the magnetic force is proportional to $\mathbf{h} \times \dot{\mathbf{n}}$, it is parallel to \mathbf{n} for any trajectory in the yz plane and has therefore no effect.
- [12] D. Loss, D. P. DiVincenzo, and G. Grinstein, Phys. Rev. Lett. **69**, 3232 (1992).
- [13] A. Garg, Europhys. Lett. **22**, 205 (1993).
- [14] V. Yu. Golyshev and A. F. Popkov, Europhys. Lett. **29**, 327 (1995).
- [15] In the dimensionless units used here, the tunneling time is of order 1. Hence, $\partial_{\tau}^2 \sim \mathcal{O}(1)$, $\dot{\phi} \sim \mathcal{O}(1)$, and obviously $\cos \phi \sim \mathcal{O}(1)$; all these terms are therefore much smaller than λ in the small-field regime.
- [16] In both the low- and high-field regimes the action is approximately equal to $4\Delta U/\omega$. Hence, our criterion also implies that the action is larger than $2\hbar$, which is also necessary for the dilute-instanton approximation to hold.
- [17] B. Barbara and E. M. Chudnovsky, Phys. Lett. A **145**, 205 (1990).
- [18] Note that this period coincides with the one obtained for the oscillations in Δ_{hf} , Eq. (5).
- [19] Note that the tunnel splitting is much larger than couplings to nuclear spins, which then cause no decoherence. Also, since each magnetic subunit is an antiferromagnet, intermolecular dipolar interactions are minimal.